

Acceleration of quantum optimal control theory algorithms with mixing strategies

Alberto Castro* and E. K. U. Gross

*Institut für Theoretische Physik and European Theoretical Spectroscopy
Facility, Freie Universität Berlin, Arnimallee 14, D-14195 Berlin, Germany*

(Dated: October 31, 2018)

Abstract

We propose the use of mixing strategies to accelerate the convergence of the common iterative algorithms utilized in Quantum Optimal Control Theory (QOCT). We show how the non-linear equations of QOCT can be viewed as a “fixed-point” non-linear problem. The iterative algorithms for this class of problems may benefit from mixing strategies, as it happens, e.g. in the quest for the ground-state density in Kohn-Sham density functional theory. We demonstrate, with some numerical examples, how the same mixing schemes utilized in this latter non-linear problem, may significantly accelerate the QOCT iterative procedures.

*Electronic address: alberto@physik.fu-berlin.de

I. INTRODUCTION

Quantum optimal control theory[1, 2, 3, 4] (QOCT) answers the following question: A system can be driven, during some time interval, by one or various external fields whose temporal dependence is determined by a set of “control” functions. Given an objective (e.g., to maximize the transition probability to a prescribed final state, the so-called target state), what are the control functions that best achieve this objective?

In the more general context of dynamical systems, optimal control theory is widely used for engineering problems, and its modern formulation was established in the 1950’s.[5] The translation of these ideas to Quantum Mechanics was initiated in the 1980’s.[6, 7, 8, 9, 10, 11, 12, 13, 14, 15, 16, 17, 18] Recently, the field has received increasing attention due to the parallel advances in experimental control techniques: femto – and atto – second laser sources with pulse shaping,[19, 20, 21] and learning loop algorithms.[22] These new developments call for corresponding theoretical efforts.

The computational solution of the QOCT equations may impose an enormous burden. Any algorithm requires multiple forward and backward propagations of the quantum system under study. This can be very cumbersome, depending on the level of theory employed to model the process. The development of efficient algorithms is therefore essential. And, in fact, rather efficient schemes already exist.[23, 24, 25, 26] The most effective choices are closely related and can be grouped in a unified framework.[27] The equations to be solved are non-linearly coupled initial-value partial differential equations, and must be solved iteratively. These iterative procedures can be described in the following way: one input field is passed to an “iteration functional” that tests its performances and produces an improved “output” field. This output field can then be used as input for the iteration functional. Upon solution, output and input fields coincide at the “fixed-point” of the iteration functional.

We must therefore search for the fixed-point of some non-linear functional. One prominent example of this kind of fixed-point problems is the Kohn-Sham (KS) formulation of density-functional theory (DFT).[28] In this field, it was soon realized that the naive use of the output produced in one iteration as input for the next one leads to poor (or no) convergence, and this observation suggested the use and development of “mixing” techniques:[29, 30, 31] the input for each iteration is a smart combination of the output of the previous iteration and several inputs or outputs of former iterations. The result is typically a very significant acceleration in the conver-

gence – and even the possibility of finding a solution in cases where no mixing (or trivial “linear” mixing) is unable of finding one.

In this work, we propose the use of those mixing strategies to accelerate the convergence of the iterative algorithms used in QOCT. We demonstrate how they can significantly reduce the iteration count – yet the performance and degree of gain, of course, depends on the details of each particular model. The procedure should be viewed as a scheme to *accelerate* (and not substitute) the existent iterative algorithms; in particular, it will be made evident that the mixing should be switched on after a couple iterations have been made and the control function is not too far away from the solution – fortunately, it is precisely the regime where the existent algorithms behave better.

The description of the proposed methodology is provided in Section II. Some numerical evidence supporting the advantages of its use is shown in Section III. Atomic units are used throughout.

II. METHODOLOGY

We recall the essential equations of QOCT, making no attempt to state them in full generality – the basic ideas can be generalized in different ways suitable for a broad class of situations; however the reader should find no difficulties to translate our suggested enhancements to those variations.

We consider a system characterized in the absence of external fields by a Hamiltonian \hat{H}_0 . One external “control” operator $\varepsilon(t)\hat{V}$ may drive it during some time interval, where $\varepsilon(t)$ is a “control function”. The system is therefore governed by:

$$\hat{H}(t) = \hat{H}_0 + \varepsilon(t)\hat{V}, \quad 0 \leq t \leq T, \quad (1)$$

which drives the system from its initial state $|\Psi_0\rangle$ to a final state $|\Psi(T)\rangle$. The purpose of the QOCT algorithms is to find that $\varepsilon(t)$ that maximizes the value of a target – in mathematical terms, a functional of the evolution of the state, $J_1[\Psi]$. In many cases it depends only on the value of the state at the end of the propagation. And in most cases it takes the form of the expectation value of some operator \hat{O} :

$$J_1[\Psi] = \langle \Psi(T) | \hat{O} | \Psi(T) \rangle. \quad (2)$$

In order to produce a physically meaningful process, the maximization of J_1 must be constrained: on one hand, one should limit the search space of ε ; on the other hand one must ensure that the evolution $|\Psi(t)\rangle$ indeed follows from Schrödinger’s equation. In mathematical terms, this

translates into the maximization of the functional:

$$J[\Psi, \chi, \varepsilon] = J_1[\Psi] + J_2[\varepsilon] + J_3[\Psi, \chi, \varepsilon], \quad (3)$$

$$J_2[\varepsilon] = -\alpha \int_0^T dt \varepsilon^2(t), \quad (4)$$

$$J_3[\Psi, \chi, \varepsilon] = -2\Im \int_0^T dt \langle \chi(t) | i \frac{d}{dt} - \hat{H}_0 - \varepsilon(t) \hat{V} | \Psi(t) \rangle. \quad (5)$$

The J_2 functional penalizes the “fluence” of the control field – ensuring that the maximization procedure does not lead to infinite values. The J_3 functional ensures that $\Psi(t)$ satisfies the Schrödinger equation, and it introduces a new “Lagrange-multiplier” wave function, χ . The Euler-Lagrange equations satisfied at the stationary points of J are:

$$i \frac{d}{dt} |\Psi(t)\rangle = [\hat{H}_0 + \varepsilon(t) \hat{V}] |\Psi(t)\rangle, \quad (6)$$

$$|\Psi(0)\rangle = |\Psi_0\rangle, \quad (7)$$

$$i \frac{d}{dt} |\chi(t)\rangle = [\hat{H}_0 + \varepsilon(t) \hat{V}] |\chi(t)\rangle, \quad (8)$$

$$|\chi(T)\rangle = \hat{O} |\Psi(T)\rangle, \quad (9)$$

$$\alpha \varepsilon(t) = \Im \langle \chi(t) | \hat{V} | \Psi(t) \rangle. \quad (10)$$

Numerous modifications and extensions to these equations are possible; for example, the possibility to include dissipation,[32] to account for multiple objectives,[33] to deal with time-dependent targets,[34, 35, 36] to add spectral and fluence constrains,[37] or to work with more general inhomogeneous integrodifferential equations of motion.[38] In order to keep the present discussion as simple as possible, we have chosen to present this “standard” set of equations, but we stress that the algorithmic enhancements discussed below may be applied to the modified versions.

The control equations (6)-(10) are coupled and one must look for a self-consistent solution. This requires an iterative scheme, which we choose to write here, for reasons that will become clear later, in “functional” form: an “iterator” F takes an input control function ε and produces an output, which is then used as input for the following iteration.

The simplest option would be what can be called a “straight iteration”: given a trial control function $\varepsilon^{(k)}$ (k is the iteration index), the output $F[\varepsilon^{(k)}]$ is constructed by taking the steps:

1. Propagate, from $|\Psi(0)\rangle = |\Psi_0\rangle$ to $|\Psi(T)\rangle$ with $\varepsilon^{(k)}$.
2. Propagate backwards, from $|\chi(T)\rangle = \hat{O} |\Psi(T)\rangle$ to $|\chi(0)\rangle$, also with $\varepsilon^{(k)}(t)$. During the evolution, calculate the output field $F[\varepsilon^{(k)}]$:

$$\alpha F[\varepsilon^{(k)}](t) = \Im \langle \chi(t) | \hat{V} | \Psi(t) \rangle. \quad (11)$$

3. Define $\varepsilon^{(k+1)} = F[\varepsilon^{(k)}]$, and repeat from step 1 until convergence is reached ($F[\varepsilon] = \varepsilon$).

This procedure was already used, for example, in the seminal work of Kosloff *et al* [13]. As discussed by Somloi *et al* [26], doing such a straight iteration in general does not lead to convergence. One possible way to cure this problem is to set $\varepsilon^{(k+1)} = \varepsilon^{(k)} + \gamma F[\varepsilon^{(k)}]$; the parameter γ may be set by performing a line-search optimization, such that $\varepsilon^{(k+1)}$ produces the maximal objective J . This idea is in fact a first-order approach to the schemes discussed below.

One monotonically convergent algorithm was introduced in Ref. [24] – we will refer to this algorithm as ZR98. It can be described in the following way: given the trial control function $\varepsilon^{(k)}$, the output $F[\varepsilon^{(k)}]$ is constructed by taking the steps:

1. Propagate, from $|\Psi(0)\rangle = |\Psi_0\rangle$ to $|\Psi(T)\rangle$ with $\varepsilon^{(k)}$.
2. Propagate backwards, from $|\chi(T)\rangle = \hat{O}|\Psi(T)\rangle$ to $|\chi(0)\rangle$, with $\tilde{\varepsilon}$ defined as:

$$\alpha\tilde{\varepsilon}(t) = \Im\langle\chi(t)|\hat{V}|\Psi(t)\rangle. \quad (12)$$

$\tilde{\varepsilon}$ must be obtained “on the fly”, from the values of the propagating $|\chi(t)\rangle$ and the previously obtained $|\Psi(t)\rangle$.

3. Propagate forward, from $|\Psi'(0)\rangle = |\Psi_0\rangle$ to $|\Psi'(T)\rangle$, using the output field $F[\varepsilon^{(k)}](t)$, which is now defined as:

$$\alpha F[\varepsilon^{(k)}](t) = \Im\langle\chi(t)|\hat{V}|\Psi'(t)\rangle. \quad (13)$$

One can then simply define $\varepsilon^{(k+1)} = F[\varepsilon^{(k)}]$, and proceed to the next iteration (note that in this case one does not need to perform explicitly step 1 again, since it repeats step 3 in the previous iteration). The solution, i.e. the optimal field, is obtained when the iteration finds a fixed point: $F[\varepsilon] = \varepsilon$.

At this point, some remarks are in order:

- The seminal algorithmic work presented in Ref. [23] deals with a slightly modified version of the previous scheme, suitable for a particular (but very common) type of target – the objective is to maximize the population of a given *target* state Ψ_{target} , and therefore the operator \hat{O} is the projection onto that state. In this case, the generating functionals can be defined in such a way that the propagations for Ψ and χ are decoupled (note that in Eqs. 6-10,

Ψ and χ are coupled through Eq. 9):

$$i \frac{d}{dt} |\Psi(t)\rangle = [\hat{H}_0 + \varepsilon(t)\hat{V}] |\Psi(t)\rangle, \quad (14)$$

$$|\Psi(0)\rangle = |\Psi_0\rangle, \quad (15)$$

$$i \frac{d}{dt} |\chi(t)\rangle = [\hat{H}_0 + \varepsilon(t)\hat{V}] |\chi(t)\rangle, \quad (16)$$

$$|\chi(T)\rangle = |\Psi_{\text{target}}\rangle, \quad (17)$$

$$\alpha \varepsilon(t) = \Im \langle \chi(t) | \hat{V} | \Psi(t) \rangle. \quad (18)$$

This algorithm, presented in Ref. 23, is essentially the same as the one defined by Eqs. 6-10, except for the fact that the initial value point for the propagation of χ is now given by Eq. 17. In the following, we will refer to this scheme as ZBR98.

- The formulation of Krotov as implemented by Tannor *et al*[25] can also be viewed as a modification of the previous scheme and, as discussed in Ref. 27, both schemes can be written as members of the same family.
- A remarkable property of both ZR98, ZBR98 and Krotov's schemes is their monotonic convergence. Also, and most importantly, they typically provide very fast improvements during the first iterations – when the trial field is very far from the solution field. Unfortunately, this rate of convergence slows down as the iteration count grows.
- The previous description of the Z(B)R98 algorithms suggests that the cost, per iteration, is that of two wave function propagations. However, this can only be possible if, at every time step in either the forward or backward step, the wave functions are stored, and then retrieved from memory when performing, respectively, the following backward or forward step. In practice, this can be time consuming, and the best way is actually to propagate once again with the same field, but in the opposite time direction. In this case, one needs, in fact, *four* propagations per iteration.

We propose now to utilize the simpler straight iteration, but with an important change: We do *not* use $\varepsilon^{(k+1)} = F[\varepsilon^{(k)}]$. Instead, we can use the sophisticated mixing algorithms that have proved so useful in the field of Kohn-Sham density functional theory,[28] such as, for example, the one presented in Ref. [30] (which we will call modified Broyden's algorithm). Other options would be equally valid – for example the work presented in Ref. [31]. One can use them exactly in the

same way as they are used in electronic structure calculations. The only external ingredient that the algorithms necessitate, and which is different for each problem, is a dot product definition for the relevant variables, which in the QOCT case are the control functions. We take the obvious choice:

$$\langle \boldsymbol{\varepsilon}_1 | \boldsymbol{\varepsilon}_2 \rangle = \int_0^T dt \boldsymbol{\varepsilon}_1(t) \boldsymbol{\varepsilon}_2(t). \quad (19)$$

In essence, the gist of Broyden's scheme (and of all of the other so-called "mixing" strategies) consists of making use, in order to define $\boldsymbol{\varepsilon}^{(k+1)}$, not only of $F[\boldsymbol{\varepsilon}^{(k)}]$, but also of a number s of previous iteration values:

$$\boldsymbol{\varepsilon}^{(k+1)} = G_{\text{mixing}}[\{ \boldsymbol{\varepsilon}^{(k-j)}, F[\boldsymbol{\varepsilon}^{(k-j)}] \}_{j=0}^{s-1}]. \quad (20)$$

The functional G_{mixing} is chosen in some way designed to minimize the distance D between input and output:

$$D(F[\boldsymbol{\varepsilon}], \boldsymbol{\varepsilon}) = \langle F[\boldsymbol{\varepsilon}] - \boldsymbol{\varepsilon} | F[\boldsymbol{\varepsilon}] - \boldsymbol{\varepsilon} \rangle^{(1/2)}. \quad (21)$$

These functionals are essentially based on approximations to the conventional Newton-Raphson iteration. Let us define $T[\boldsymbol{\varepsilon}] = F[\boldsymbol{\varepsilon}] - \boldsymbol{\varepsilon}$; in the vicinity of $\boldsymbol{\varepsilon}^{(k)}$ (the k -th iteration approximation to the solution), the functional T can be linearized:

$$T[\boldsymbol{\varepsilon}] \approx T[\boldsymbol{\varepsilon}^{(k)}] + J^{(k)}[\boldsymbol{\varepsilon} - \boldsymbol{\varepsilon}^{(k)}], \quad (22)$$

where $J^{(k)}$ is the Jacobian of T evaluated at $\boldsymbol{\varepsilon}^{(k)}$. This can be rewritten as:

$$\boldsymbol{\varepsilon} - \boldsymbol{\varepsilon}^{(k)} + G^{(k)}[T[\boldsymbol{\varepsilon}] - T[\boldsymbol{\varepsilon}^{(k)}]] = 0, \quad (23)$$

where $G^{(k)} = -(J^{(k)})^{-1}$. Newton's iteration follows immediately from this formula by assuming $\boldsymbol{\varepsilon}^{(k+1)}$ to be the solution vector ($T[\boldsymbol{\varepsilon}^{(k+1)}] = 0$):

$$\boldsymbol{\varepsilon}^{(k+1)} = \boldsymbol{\varepsilon}^{(k)} + G^{(k)}[T[\boldsymbol{\varepsilon}^{(k)}]]. \quad (24)$$

Since the Jacobian (let alone its inverse) may be difficult to compute, *quasi* Newton-Raphson schemes utilize approximations to it; in Broyden's family of schemes, these are also built iteratively. Therefore, the matrices $G^{(k)}$ do not verify Eq. 23 until convergence.

Johnson's proposal,[30] in particular, consists of generating $G^{(k+1)}$ by minimizing the following functional:

$$E = \omega_0^2 \|G^{(k+1)} - G^{(k)}\|^2 + \sum_{n=1}^k \omega_n^2 |\Delta \boldsymbol{\varepsilon}^{(n)} + G^{(k+1)} \Delta T^{(n)}|^2, \quad (25)$$

where $\Delta\boldsymbol{\varepsilon}^{(n)} = \boldsymbol{\varepsilon}^{(n+1)} - \boldsymbol{\varepsilon}^{(n)}$, $\Delta T^{(n)} = T[\boldsymbol{\varepsilon}^{(n+1)}] - T[\boldsymbol{\varepsilon}^{(n)}]$, and ω_i are a set of real positive constant weights. The idea is therefore to minimize the error in the inverse Jacobian (first term in the definition of E), at the same time making sure that the new guess for G verifies Eq. 23 as closely as possible – not only for the last iteration $\boldsymbol{\varepsilon}^{(k)}$, but also for all the previous ones.

The minimization of E with respect to $G^{(k+1)}$ leads to an iterative formula; this formula can then be plugged into Eq. 24. The final result reads:

$$\boldsymbol{\varepsilon}^{(k+1)} = \boldsymbol{\varepsilon}^{(k)} + G^{(1)}T[\boldsymbol{\varepsilon}^{(k)}] - \sum_{n=1}^{k-1} \omega_n \gamma_{kn} u^{(n)}, \quad (26)$$

where:

$$u^{(n)} = G^{(1)}\Delta T^{(n)} + \Delta\boldsymbol{\varepsilon}^{(n)}, \quad (27)$$

$$\gamma_{kl} = \sum_{n=1}^{k-1} \omega_n \langle \Delta T^{(n)} | T^{(k)} \rangle \beta_{nl}, \quad (28)$$

$$\beta_{nl} = (\omega_0^2 I + a)_{nl}^{-1}, \quad (29)$$

$$a_{ij} = \omega_i \omega_j \langle \Delta T^{(j)} | \Delta T^{(i)} \rangle. \quad (30)$$

In this manner, the new field $\boldsymbol{\varepsilon}^{(k+1)}$ can be obtained from information gathered in the previous iterations; it only remains to choose an appropriate initial guess for the inverse Jacobian, $G^{(1)}$; we merely set it equal to some constant times the identity, αI . This constant α can be freely chosen (it ultimately determines the amount of “output” field to be utilized in the mixture, as it can be understood inspecting Eq. 26), and it is a matter of experience to determine a reasonable value – likewise for the ω_i constants. In typical DFT codes, the ω_i constants are not adjusted for each run; the same values are used for all systems. α is usually set initially to some “aggressive” value (i.e. large value, meaning a large proportion of the “output” is used), and, if convergence is not found, it is reduced in a subsequent run. We expect that the same strategy should hold for QOCT runs.

A careful analysis of Eq. 26 also reveals that we do not need to manipulate or store objects of size N^2 , where N is the dimension of the problem field $\boldsymbol{\varepsilon}$. The cost of the operations is of order sN , where s is the number of previous iterations to be considered in the formula. This is the key reason to utilize this modification of Broyden’s scheme, since in a typical QOCT problem the dimension N is given by the number of time steps in the propagation, which can be easily of the order of 10^6 .

Regarding numerical details, we have implemented the QOCT machinery in our electronic-structure `octopus` code.[39] Since one of the tasks of this code is to solve the KS DFT problem, the mixing strategies cited above are implemented. This platform is specialized in the time-dependent

version of DFT, TDDFT, and therefore contains sophisticated time-propagation schemes,[40] utilized for the results shown below. We have recently employed our QOCT machinery – without making use of the mixing strategies – to model the control of electrons trapped in two dimensional semiconductor quantum nanostructures.[41]

III. RESULTS

A. Asymmetric double well

As a first example, we will use a simple, but prototypical example: the transfer of a wave packet from one to another well in an asymmetric double well potential. The field-free Hamiltonian is:

$$\hat{H}_0 = -\frac{1}{2} \frac{\partial^2}{\partial x^2} + \frac{x^4}{64} - \frac{x^2}{4} + \frac{x^3}{256}. \quad (31)$$

The potential is depicted on top of Fig. 1. Qualitatively similar potentials appear in many areas in Physics, and in Quantum Chemistry they are sometimes used to model isomerization problems.[42] The external control couples to the system through the dipole operator: $\hat{V} = -\hat{x}$.

The ground state, Ψ_g is localized in the left, deeper, well. The first excited state, which will be our target, Ψ_{target} , is localized in the right well. These states are also depicted in Fig. 1. The target operator \hat{O} is in this case the projection $|\Psi_{\text{target}}\rangle\langle\Psi_{\text{target}}|$, and therefore the preferred algorithm to start with is the one presented in Ref. [23], ZBR98. In addition, we will use straight iteration assisted by Broyden’s mixing.

Fig. 2 displays four QOCT runs, each of them considering a different initial guess for the solution field:

$$\varepsilon^{(0)}(t) = E_0 \cos(\omega t). \quad (32)$$

We try the optimization with four different values of E_0 , as displayed on each of the panels. Both the values of the total functional J and of the objective J_1 are displayed. Before describing the results, we should point out that, as discussed above, there are some adjustable parameters to completely define the mixing algorithm: (i) the number s of previous iterations considered in the construction of the algorithm – which is set to four in this case; (ii) a number α that specifies the amount of output field, $\alpha F[\varepsilon^{(k)}]$, that is utilized in the mixing – we use $\alpha = 0.1$; (iii) also, it is sometimes advisable to stop the algorithm every given number of steps, and restart erasing the memory from previous iterations – in Fig. 2, however, we have chosen to put the straightforward algorithm. We have made no attempt to optimize the method by taking advantage of this freedom.

The results are very promising: except for the case (top left) where the initial laser field has very low amplitude ($E_0 = 0.01$), leading to a very small initial overlap J_1 , in all the other cases Broyden’s mixing converges faster – and in fact converges to a different, better maximum. Unfortunately, the exception in the top left corner is very disappointing since the procedure yields the zero field – which is also a solution of the QOCT equations, but certainly not the desired one.

And that exception is indeed specially important, since it exemplifies an important weakness of using straight iteration together with Broyden’s algorithm: the algorithm behaves very poorly if the initial guess is not good enough. Fortunately, this is precisely the regime where most of the already existent algorithms behave better – and therefore one can devise a “hybrid” procedure: a few iterations with, for example, ZBR98, followed by the mixing iterations. Fig. 3 displays the results obtained in this way: at iteration number three, the ZBR98 procedure is stopped. Then, after a couple of irregular iterations (that irregularity can however be controlled by a more careful selection of the parameter α mentioned above), the results are significantly better.

B. Morse potential

For our second example, we have chosen a case that has already been discussed in the literature: the vibrational excitations in a Morse potential model for the OH bond. This potential function is given by: [43]

$$V(x) = D_0 [\exp(-\beta(x - r_0)) - 1]^2 - D_0, \quad (33)$$

where, for the OH case, the parameters are chosen to be: $D_0 = 0.1994$, $\beta = 1.189$, $r_0 = 1.821$. The coupling to the external function is given now by a dipole potential operator approximated by the function:

$$V(x) = \mu_0 x \exp(-x/r^*), \quad (34)$$

where $\mu_0 = 3.088$ and $r^* = 0.6$. The objective is now to populate the first excited state, starting from the Morse ground state. The total propagation time is $T = 30000$ a.u. (≈ 0.725 ps); the initial trial input field is the zero field, and the penalty factor is $\alpha = 1$. This is precisely the first example discussed by Zhu *et al* [23] to demonstrate the performance of the ZBR98 algorithm. We have replicated those calculations with our codes, and in the following we demonstrate how the addition of mixing strategies significantly boosts the performance of the original scheme. [44]

The results are shown in Fig. 4. First of all, we should note that the attempt to apply a straight iteration scheme right from the zero-th iteration – whether or not assisted by mixing techniques –

will fail, since the initial input field is already a solution to the QOCT equations. This solution, however, is an unstable point, and the ZBR98 in this case relies on numerical error to abandon this unstable solution, and then proceeds until convergence into a maximum. The behavior of this algorithm is summarized by the circles in Fig. 4, which show both the values of J_1 and J at each iteration step. These results are almost exactly the same as the ones given in Ref. 23. Also, the final converged field (shown in the inset of Fig. 4) coincides with the one reported in that work.

In order to speed up the convergence, we utilized the modified Broyden’s mixing algorithm to accelerate the straight iteration scheme, starting from the field obtained after the first ZBR98 iteration. The results are shown in Fig. 4 with squares; the thick black curve in particular refers to the convergence of the J functional. It may be seen how the final converged value, $J(\infty) = 0.885$, is obtained in a few iterations. In order to achieve the same level of convergence, ZBR98 necessitates around 50 iterations. Once again, it should be noted that in a usual implementation, each straight iteration step will be half as costly as a ZBR98 step.

IV. CONCLUSIONS

To summarize, ideas borrowed from a particular field of computational physics (e.g., density functional theory techniques) have been used successfully in the completely different context of QOCT algorithms. The reason for success is, of course, the underlying parallelism in the equations, if regarded with the appropriate “abstract eye”.

This work by no means proves, in mathematical rigour, the universal advantage of using mixing strategies for all QOCT problems. However, we have observed important speedups in most cases (as in the ones presented in this article), and we feel that the analogy with the KS DFT problem provides convincing evidence about the usefulness of employing mixing for QOCT. Two important features of previous algorithms are, unfortunately, lost: the monotonic convergence (this could be cured, nevertheless, by adapting the mixing scheme proposed by Bowler and Gillan [31]), and the usual large gains during the first iterations when the initial guess is far from the solution.

This excellent performance of both Z(B)R98 or Krotov’s algorithm for the first iterations suggests the use of the mixing schemes not as a substitute, but as a complement – as demonstrated in our sample runs. Moreover, we should note that the idea of mixing several iterative steps according to, e.g., Broyden’s scheme can also be applied *on top of* the usual ZBR98, ZR98 or Krotov’s algorithms (and not on top of the straight iteration scheme, as it has been presented here). Our

experience shows that, in most cases, doing this accelerates the convergence – although at the cost of losing the predictable, regular, monotonic behaviour. Finally, we remark that the suggested algorithms can be easily mounted on top of the already working programs.

Acknowledgements

We acknowledge support by the EC Network of Excellence NANOQUANTA (NMP4-CT-2004-500198), and by the Deutsche Forschungsgemeinschaft within the SFB 450.

-
- [1] H. Rabitz, R. de Vivie-Riedle, M. Motzkus and K. Kompa, *Science* **288**, 824 (2000).
 - [2] S. A. Rice and M. Zhao, *Optical Control of Molecular Dynamics* (John Wiley & Sons, New York, 2000).
 - [3] M. Shapiro and P. Brumer, *Principles of the Quantum Control of Molecular Processes*, (Wiley, New York, 2003).
 - [4] J. Werschnik and E. K. U. Gross, *J. Phys. B: At. Mol. Opt. Phys.* **40**, R175 (2007); J. Werschnik, *Quantum Optimal Control Theory: Filter Techniques, Time-Dependent Targets, and Time-Dependent Density-Functional Theory*, (Curvillier Verlag, Göttingen, 2006).
 - [5] See, e.g., D. G. Luenberger, *Introduction to Mechanical Systems*, (John Wiley & Sons, New York, 1979).
 - [6] S. Shi, A. Woody, and H. Rabitz, *J. Chem. Phys.* **88**, 6870 (1988).
 - [7] S. Shi and H. Rabitz, *Chem. Phys.* **139**, 185 (1989).
 - [8] A. P. Peirce, M. A. Dahleh and H. Rabitz, *Phys. Rev. A* **37**, 4950 (1988).
 - [9] R. S. Judson, K. K. Lehmann, H. Rabitz, and W. S. Warren, *J. Mol. Struct.* **223**, 425 (1990).
 - [10] M. Dahleh, A. P. Peirce, and H. Rabitz, *Phys. Rev. A* **42**, 1065 (1990).
 - [11] K. Yao, S. Chi, and H. Rabitz, *Chem. Phys.* **150**, 373 (1990).
 - [12] D. J. Tannor and S. A. Rice, *Adv. Chem. Phys.* **70**, 441 (1988).
 - [13] R. Kosloff, S. A. Rice, P. Gaspard, S. Tersigni and D. J. Tannor, *Chem. Phys.* **139**, 201 (1989).
 - [14] S. H. Tersigni, P. Gaspard, and S. A. Rice, *J. Chem. Phys.* **93**, 1670 (1990).
 - [15] D. J. Tannor, in *Molecules in Laser Fields*, edited by A. D. Bandrauk (Marcel Dekker, New York, 1994), p. 403.

- [16] W. Jakubetz, J. Manz, and V. Mohan, *J. Chem. Phys.* **90**, 3686 (1989).
- [17] J. E. Combariza, B. Just, J. Manz, and G. K. Paramonov, *J. Phys. Chem.* **95**, 10351 (1991).
- [18] A. Butkovskii and Y. Samoilenko, *Control of Quantum-Mechanical Processes and Systems*, (Kluwer Academic, Dordrecht, 1990).
- [19] A. M. Weiner, *Rev. Sci. Instrum.* **71**, 1929 (2000).
- [20] T. Brixner, G. Krampert, T. Pfeifer, R. Selle, G. Gerber, M. Wollenhaupt, O. Graefe, C. Horn, D. Liese and T. Baumert, *Phys. Rev. Lett.* **92**, 208301 (2004).
- [21] M. Y. Shverdin, D. R. Walker, D. D. Yavuz, G. Y. Yin and S. E. Harris, *Phys. Rev. Lett.* **94**, 033904 (2005).
- [22] R. Judson and H. Rabitz, *Phys. Rev. Lett.* **68**, 1500 (1992).
- [23] W. Zhu, J. Botina and H. Rabitz, *J. Chem. Phys.* **108**, 1953 (1998).
- [24] W. Zhu and H. Rabitz, *J. Chem. Phys.* **109**, 385 (1998).
- [25] D. J. Tannor, V. Kazakov and V. Orlov, in *Time Dependent Quantum Molecular Dynamics*, edited by J. Broeckhove and L. Lathouwers (Plenum, New York, 1992), pp. 347-360.
- [26] J. Somloi, V. A. Kazarov and D. J. Tannor, *Chem. Phys.* **172**, 85 (1993).
- [27] Y. Maday and G. Turinici, *J. Chem. Phys.* **118**, 8191 (2003).
- [28] R. M. Dreizler and E. K. U. Gross, *Density Functional Theory. An Approach to the Quantum Many Body Problem*, (Springer-Verlag, Berlin, 1990); Fiolhais, F. Nogueira and M. A. L. Marques, editors, *A Primer in Density Functional Theory*, Lecture Notes in Physics 620, (Springer Verlag, Berlin, 2003).
- [29] D. G. Anderson, *J. Assoc. Comput. Mach.* **12**, 547 (1964); P. Pulay, *Chem. Phys. Lett.* **73**, 393 (1980). P. Pulay, *J. Comp. Chem.* **3**, 556 (1982); C. G Broyden, *Math. Comp.* **19**, 577 (1965).
- [30] D. D. Johnson, *Phys. Rev. B* **38**, 12807 (1988).
- [31] D. R. Bowler and M. J. Gillan, *Chem. Phys. Lett.* **325**, 473 (2000).
- [32] Y. Ohtsuki, W. Zhu and H. Rabitz, *J. Chem. Phys.* **110**, 9825 (1999).
- [33] Y. Ohtsuki, K. Nakagami, Y. Fujimura, W. Zhu and H. Rabitz, *J. Chem. Phys.* **114**, 8867 (2001).
- [34] Y. Ohtsuki, G. Turinici and H. Rabitz, *J. Chem. Phys.* **120**, 5509 (2004).
- [35] A. Kaiser and V. May, *J. Chem. Phys.* **121**, 2528 (2004).
- [36] I. Serban, J. Werschnik and E. K. U. Gross, *Phys. Rev. A* **71**, 053810 (2005).
- [37] J. Werschnik and E. K. U. Gross, *J. Opt. B: Quantum Semiclass. Opt.* **7**, S300 (2005).
- [38] Y. Ohtsuki, Y. Teranishi, P. Saalfrank, G. Turinici and H. Rabitz, *Phys. Rev. A* **75**, 033407 (2007).
- [39] M. A. L. Marques, A. Castro, G. F. Bertsch and A. Rubio, *Comp. Phys. Comm.* **151**, 60

- (2003); A. Castro *et al*, *phys. stat. sol. (b)* **243**, 2465 (2006). The code is freely available at <http://www.tddft.org/programs/octopus/>.
- [40] A. Castro, M. A. L. Marques, and A. Rubio, *J. Chem. Phys.* **121**, 3425 (2004).
- [41] E. Räsänen, A. Castro, J. Werschnik, A. Rubio and E. K. U. Gross, *Phys. Rev. Lett.* **98**, 157404 (2007);
E. Räsänen, A. Castro, J. Werschnik, A. Rubio and E. K. U. Gross, *Physica E* **40**, 1593 (2008).
- [42] N. Džslić, O. Kühn, J. Manz and K. Sundermann, *J. Phys. Chem. A* **102**, 9645 (1998).
- [43] P. M. Morse, *Phys. Rev.* **34**, 57 (1929); G. K. Paramonov, *Chem. Phys.* **177**, 169 (1993).
- [44] In order to replicate exactly the calculations presented in Ref. 23 (Figs. 1 to 4), we have employed the same parameters quoted in that paper. However, in our opinion, the values of μ_0 and r_0 should be 1.634 and 1.134, respectively, and not the numbers that have been used. The correct numbers are given, for example, in: W. Jakubetz, J. Manz, and V. Mohan, *J. Chem. Phys.* **90**, 3686 (1989); H. P. Breueur, K. Dietz, and M. Holthaus, *J. Phys. B: At. Mol. Opt. Phys.* **24**, 1343 (1991).

List of Figures

| | | |
|---|--|----|
| 1 | Asymmetric potential well (thick line), together with the initial (dotted line) and target (dashed line) states. | 16 |
| 2 | Convergence histories for both the ZBR98 algorithm and the straight iteration scheme assisted with the modified Broyden mixing scheme. Each panel displays the results obtained with a different initial guess (see text). | 17 |
| 3 | Convergence histories for both the ZBR98 algorithm and the straight iteration scheme assisted with the modified Broyden mixing scheme. The modified Broyden scheme, however, is only applied after the third iteration. | 18 |
| 4 | Convergence histories for both the ZBR98 algorithm (lines with circles) and for the straight iteration scheme assisted with the modified Broyden mixing scheme (lines with squares), for the case of the Morse potential. Both the values for the J_1 (“target functional”, lower lines) and for the total J functional (upper lines) are shown. Inset: optimized control field. | 19 |

Figures

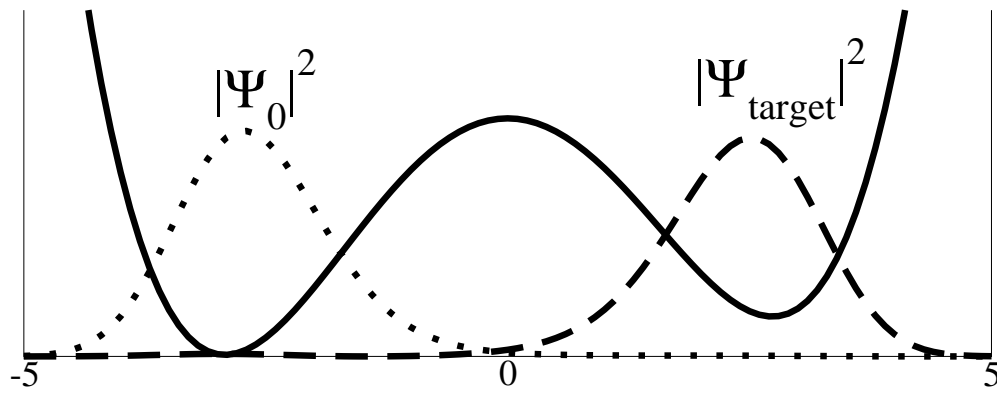


FIG. 1: Asymmetric potential well (thick line), together with the initial (dotted line) and target (dashed line) states.

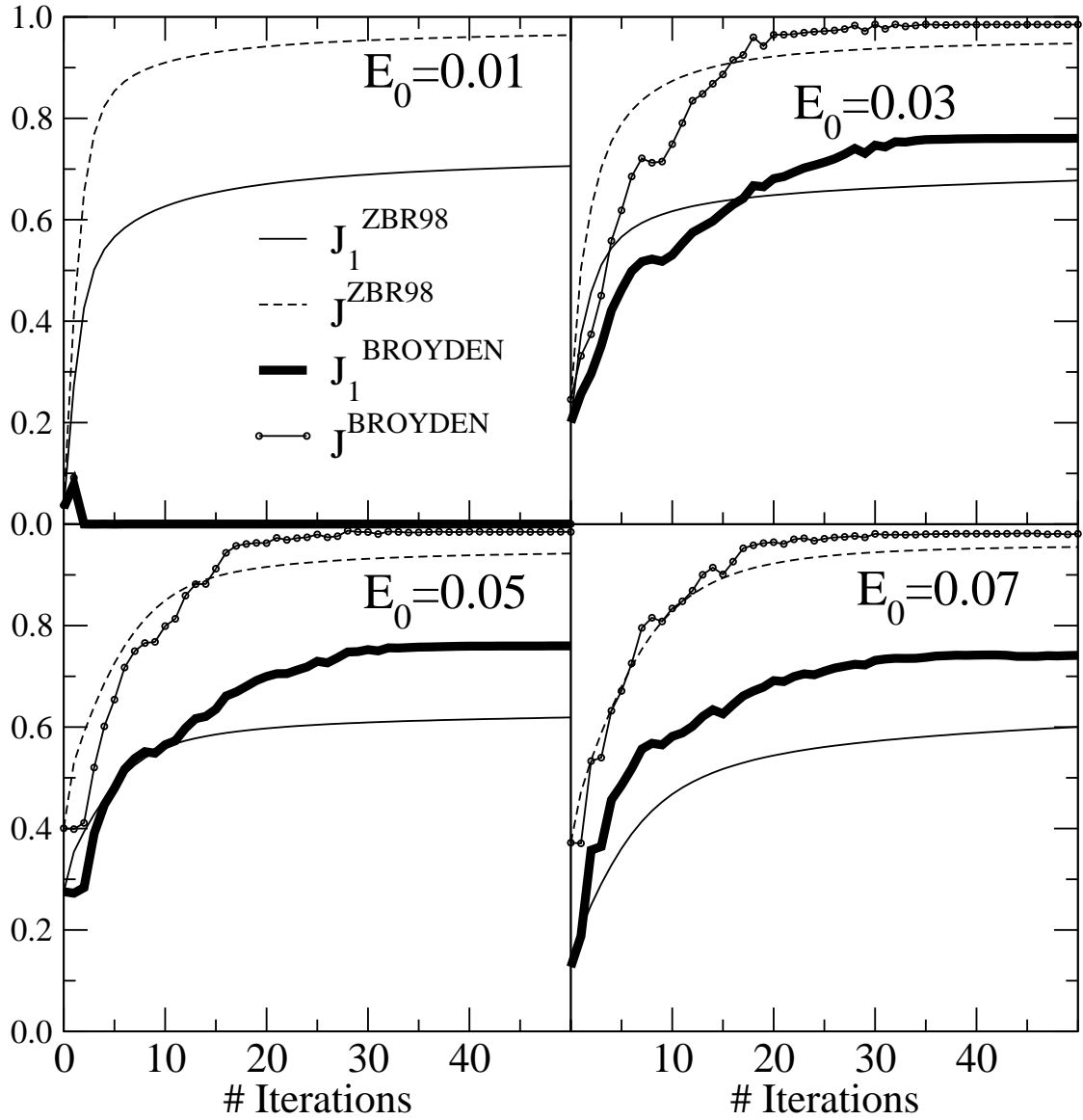


FIG. 2: Convergence histories for both the ZBR98 algorithm and the straight iteration scheme assisted with the modified Broyden mixing scheme. Each panel displays the results obtained with a different initial guess (see text).

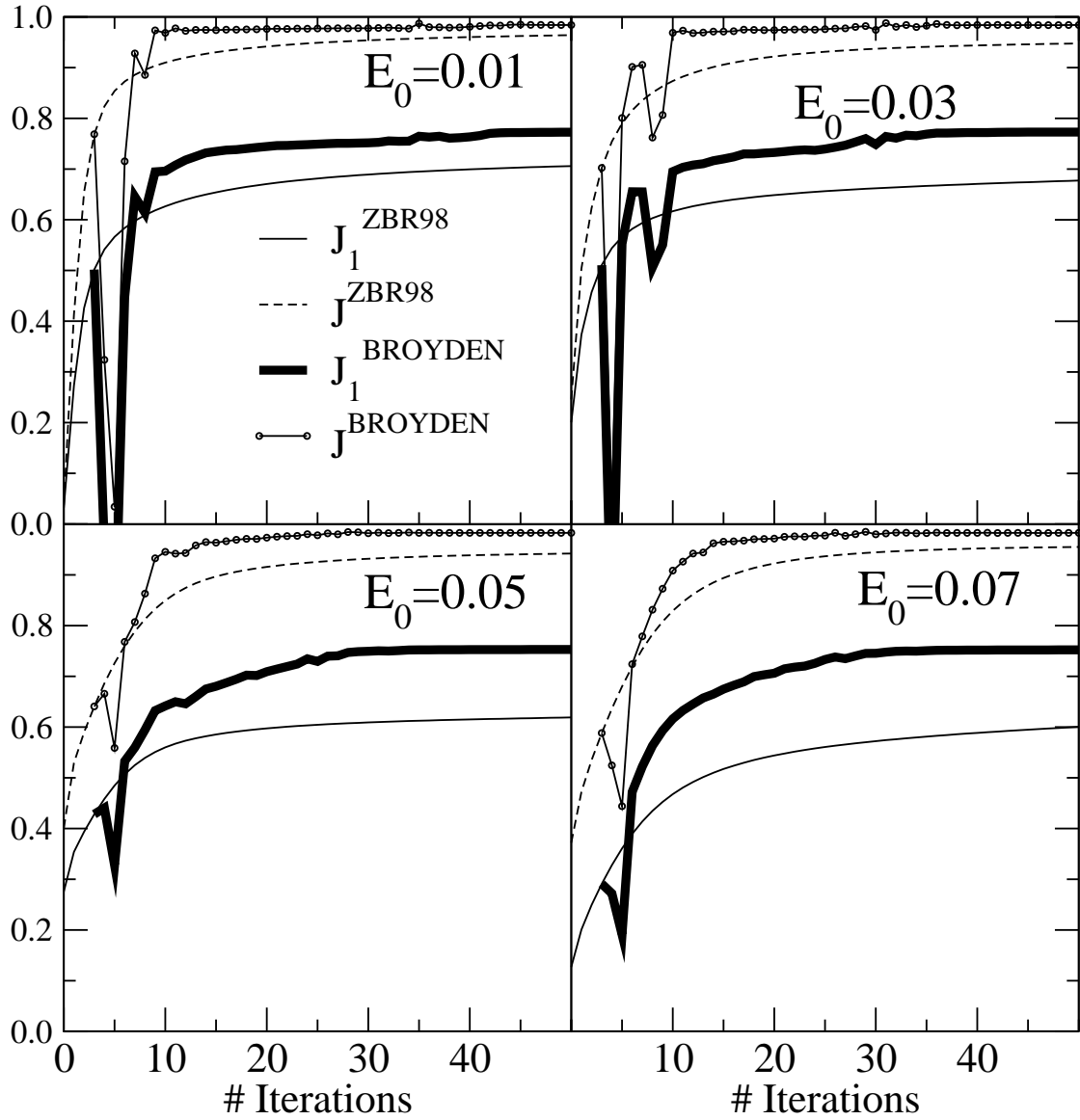


FIG. 3: Convergence histories for both the ZBR98 algorithm and the straight iteration scheme assisted with the modified Broyden mixing scheme. The modified Broyden scheme, however, is only applied after the third iteration.

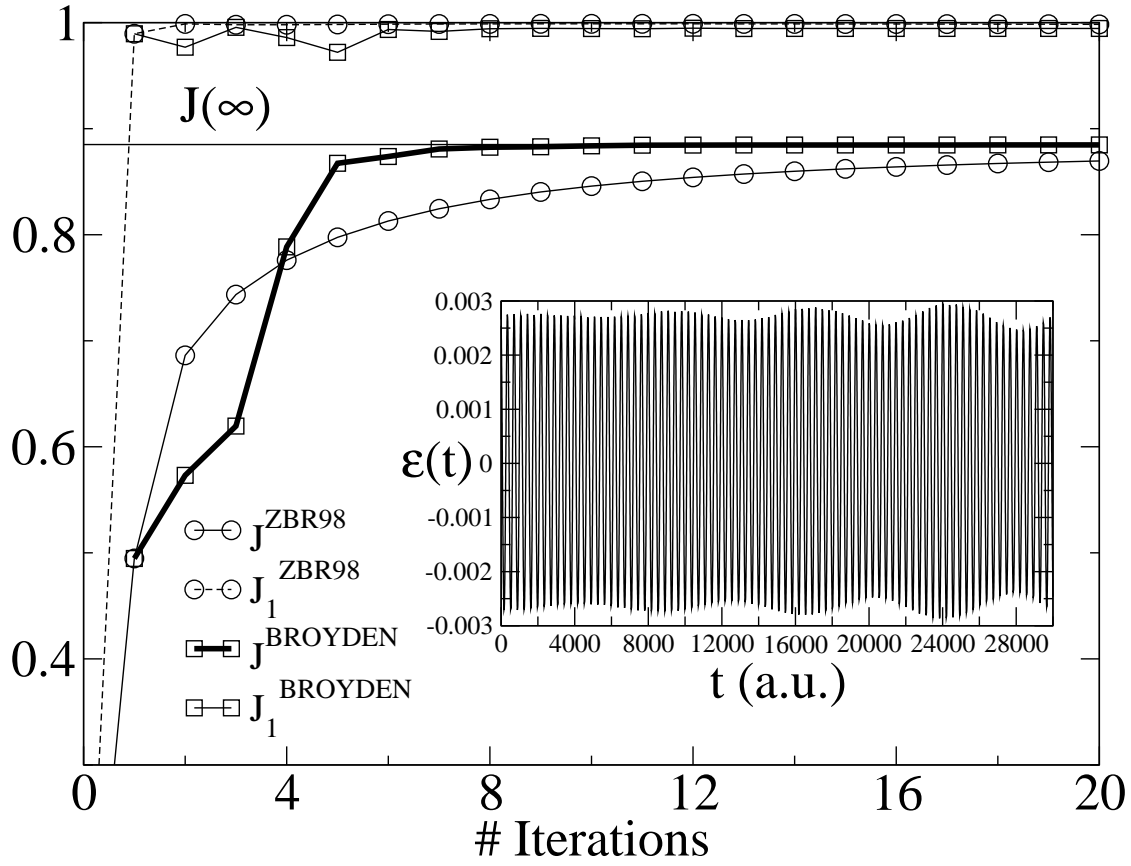


FIG. 4: Convergence histories for both the ZBR98 algorithm (lines with circles) and for the straight iteration scheme assisted with the modified Broyden mixing scheme (lines with squares), for the case of the Morse potential. Both the values for the J_1 (“target functional”, lower lines) and for the total J functional (upper lines) are shown. Inset: optimized control field.